2º CONGRESSO BRASILEIRO DE P&D EM PETRÓLEO & GÁS

POROSITY OF PACKED BEDS OF SPHEROCYLINDERS USING THE MONTE CARLO METHOD

Charlles R. A. Abreu, Frederico W. Tavares, Marcelo Castier

Escola de Química, Universidade Federal do Rio de Janeiro, Caixa Postal 68542, Rio de Janeiro, RJ, 21949-900, Brazil,
E-mail: castier@eq.ufrj.br

Resumo – Aplicações de materiais granulares, tais como leitos fixos de partículas, são freqüentes no setor de petróleo e gás. Sólidos granulares podem também ser utilizados como adsorventes para armazenamento de gás natural em veículos. Portanto, o conhecimento de propriedades destes materiais é importante para um projeto de equipamentos seguro e eficiente. Neste trabalho, de forma a se avaliar a influência do formato das partículas sobre a porosidade de leitos de partículas, configurações de leitos monodispersos de esferocilindros de mesmo volume, mas com diferentes alongamentos, são obtidas através do método de Monte Carlo.

Palavras-Chave: leitos de partículas; Monte Carlo; porosidade; esferocilindros

Abstract – Applications of granular materials, such as packed particle beds, are frequent in the oil and gas sector. Granular solids can also be used as adsorbents for natural gas storage in vehicles. Therefore, knowledge of the properties of such materials is important for safe and efficient equipment design. In this work, in order to evaluate the influence of particle shape on the porosity of particle beds, configurations of monodispersed beds of spherocylinders with equal volume, but different elongations, are obtained using the Monte Carlo method.

Keywords: particle beds, Monte Carlo, porosity, spherocylinders

1. Introduction

Granular materials are present in a wide range of industrial applications. Even in plants for fluid processing, as those in the oil and gas industry, they are located inside certain pieces of equipment, such as catalytic reactors, filters, and packed columns. Granular solids can also be used as adsorbents for natural gas storage in vehicles (Matranga et al., 1992; Wegrzyn and Gurevich, 1996). As an alternative to compression, this process has the advantage of its lower operating pressure. According to Wegrzyn and Gurevich (1996), this characteristic reduces refueling costs as well as safety risks and, additionally, allows the use of conformable tanks. In any case, efficient and safe equipment design requires knowledge of structural properties of the systems.

Rosato et al. (1986) were pioneers in applying the Monte Carlo Method for simulating particle beds. Using a technique to simulate shaking, they studied size segregation occurring in two-dimensional mixtures of hard disks. Castier et al. (1998) extended such work for three-dimensional systems of quasi-hard spheres. Abreu et al. (1999) performed Monte Carlo simulations for obtaining packed bed configurations of hard spheres. Calculated radial void fraction profiles showed good agreement with experimental data found in the literature.

Since all the previous work using Monte Carlo methods for simulating either packing or segregation concern only to spherical particles, it was not possible to evaluate the influence of particle shape on such phenomena. The present work aims at the development of a Monte Carlo method for simulating three-dimensional granular systems of non-spherical particles. The particle model is the rigid spherocylinder, that is, a convex body composed of a cylinder with two hemispheres at its edges. Some authors, such as Bolhuis and Frenkel (1997), for example, have already used this model in Monte Carlo simulations of fluids. The reason of this choice is that spherocylinders can vary from spheres to rod-like particles, depending on their aspect ratios. Besides, there is an efficient algorithm for detecting overlaps among them (Vega and Lago, 1994), what is crucial for rigid particle Monte Carlo simulations. Applying the developed method, relations between the porosity of monodispersed beds of spherocylinders and the aspect ratio of the particles are obtained. Using a technique similar to that proposed by Rosato et al. (1986) for simulating mechanical shaking, the effect of the vibration amplitude on the final configurations are evaluated. The results can be applied for enhancing efficiency in vehicular natural gas storage systems.

2. Formulation

2.1. Particle Model

Although the systems considered in this work are three-dimensional, it is easier to represent a particle in two dimensions, as in Figure 1. Considering a system with N_P particles, the diameter of a certain particle "i" is equal to σ_i and the length of its cylindrical portion is equal to ℓ_i. A vector $\mathbf{r}_i$ gives the spatial position of its center while a unit vector $\mathbf{u}_i$ represents its orientation. Therefore, a configuration of such system is a set of values for all these parameters. The aspect ratio of a particle "i" (φ_i) is defined as the ratio between ℓ_i and σ_i. Therefore, a sphere is a spherocylinder with null aspect ratio. For further calculations, it is also convenient to define the shaft of a spherocylinder as the main axis of its cylindrical portion, represented in Figure 1 by the dotted line.

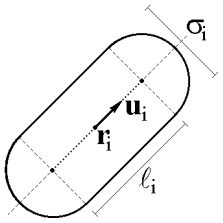

Figure 1. 2D Representation of a spherocylinder

2.2. The Monte Carlo Method

Starting from an initial configuration, the Monte Carlo Method (Allen and Tildesley, 1987) consists of a Markovian sequence of transitions in which small changes in the positions and/or orientations of the particles are proposed, one at a time, in order to sample configurational states of the system. For a canonical ensemble, all these configurations have the same temperature (T), volume (V) and number of particles (N_P). In this case, the probability of accepting the transition from an old state to a new one is

$$P_{O\to N} = \min\left[1, \exp\left(-\frac{\Delta E}{kT}\right)\right] \tag{1}$$

where ΔE is the difference between the configurational energies of the new and old states [$E^{(N)}$-$E^{(O)}$], k is the Boltzmann's constant and T is the system temperature.

The trials run in order of the particle indexes. First, a particle "i" undergoes a random displacement around its current position. Then, the acceptation or rejection of the new configurational state depends on the probability given by Equation (1). After that, if this particle is not a sphere, it is necessary to account for a small random rotation. Such rotation occurs around one of the Cartesian axes (x, y or z), randomly chosen, with a random angle constrained in the interval $[-\theta_{max,i}, \theta_{max,i}]$ (Allen and Tildesley, 1987). Again, the acceptation/rejection of the transition follows Equation (1). It is assumed that this procedure takes the system to thermodynamic equilibrium (Allen and Tildesley, 1987). In this work, the Monte Carlo Method is, in fact, a tool for obtaining mechanically stable configurations of packed beds of spherocylinders. Abreu et al. (1999) used the same methodology for the case of spherical particles, based on the work of Castier et al. (1998). These articles present the details and considerations about this kind of application. Only some additional features are presented here.

2.4 Configurational Energy Calculation

The total potential energy (E) of a system takes into account the contribution of external fields on each particle as well as of particle-particle interactions. In this work, the considered fields are gravity, buoyancy, and interaction with container walls. The expression for the configurational energy is

$$E = \sum_{i=1}^{N_P} v_i (\rho_i - \rho_f) g r_{iz} + \sum_{i=1}^{N_P} E_i^w + \sum_{i=1}^{N_P - 1} \sum_{j=i+1}^{N_P} E_{ij} \tag{2}$$

where ρ_i is the density of a particle "i" and r_{iz} is the component z of its vector $\mathbf{r}_i$. Variable ρ_f denotes the fluid density, while g is the gravity acceleration. The variable E_i^w represents the potential energy imposed on a particle "i" by the container walls and E_{ij} is the energy of the interaction between two particles "i" and "j". For calculating the volume of a particle "i", denoted in the above equation by v_i, one can use the following expression:

$$v_i = \frac{\pi \sigma_i^3}{6} \left(1 + \frac{3}{2} \varphi_i \right) \tag{3}$$

All the considered simulation boxes in this work have flat rigid walls at their tops and bottoms. In the lateral directions, some boxes have cylindrical walls, while the others present periodic boundary conditions. The use of the first box kind aims at the observation of wall effects on the particle beds, while the use of the second kind has the purpose of calculating bulk properties. Since the container walls are rigid, the potential energy of a system becomes infinite if a particle overlaps any one of them. For a cylindrical box, the potential energy of a particle "i" due to the presence of the simulation box walls (E_i^w) is (Abreu, 2002)

$$E_i^w = \begin{cases} 0 & \text{if} \quad \Delta_{iz} < \dfrac{H - \sigma_i}{2} \quad \text{and} \quad \Delta_{ir} < \dfrac{D - \sigma_i}{2} \\ \infty & \text{otherwise} \end{cases} \tag{4}$$

where H and D are, respectively, the height and the diameter of the simulation box. The variables Δ_{iz} and Δ_{ir} are the longest distances between the shaft of the particle "i" and, respectively, the plane xy and the axis z. Such variables are obtained by (Abreu, 2002)

$$\Delta_{iz} = |r_{iz}| + \frac{\ell_i}{2} |u_{iz}| \quad \text{and} \quad \Delta_{ir} = \sqrt{r_{ix}^2 + r_{iy}^2 + \frac{\ell_i^2}{4} \left(u_{ix}^2 + u_{iy}^2 \right) + \ell_i \left| u_{ix} r_{ix} + u_{iy} r_{iy} \right|} \tag{5}$$

If periodic boundary conditions apply in the lateral directions, instead of a cylindrical wall, one may consider only the term corresponding to the top and bottom walls (where Δ_{iz} appears) in the calculation of the potential energy. In this case, the cross-section of the simulation box is a square and the symbol L represents its side length. The last term of Equation (2) accounts for the contribution of particle-particle interactions. Since the particles are rigid and do not attract each other, the potential energy of interaction between two particles "i" and "j" is infinite if they are overlapping and zero if they are not. Figure 2 shows an example, in two dimensions, of a contact between two spherocylinders. Such contact happens if the shortest distance between their shafts (δ_{ij}) is equal to the sum of their radii. In other words, the pair potential (E_{ij}) of hard spherocylinders is the following:

$$E_{ij} = \begin{cases} 0 & \text{if} \quad \delta_{ij} > \dfrac{\sigma_i + \sigma_j}{2} \\ \infty & \text{otherwise} \end{cases} \tag{6}$$

For evaluating the variable δ_{ij}, a fast algorithm proposed by Vega and Lago (1994) is used.

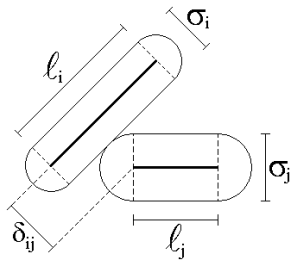

Figure 2. Contact between two spherocylinders

2.5 Mechanical Vibrations

The methodology used here to account for the vibrations is similar to that of Rosato et al. (1986), but with some precautions. In every shaking step, as a way of promoting an initial expansion of the particle assembly, the system undergoes, at first, a certain number of Monte Carlo cycles (N_{min}). Then, the convergence of the settling process (reaching of minimum energy) must be checked while the simulation goes on, what is made by comparing average energy values calculated from time to time. In this work, the final configurations of N_{avg} successive Monte Carlo cycles are used to compute each average. The settling process stops when the relative difference between two consecutively calculated averages is lower than a certain tolerance δ_E. Finally, all the particles are simultaneously lifted through the addition of a fixed value A_{vib}, which represents the vibration amplitude, to every vector-component . It is worth remarking that many transitions can be rejected in a single Monte Carlo step, causing a very small variation in the energy of two consecutive cycles. Therefore, the values of N_{min} and N_{avg} must be sufficiently high to prevent a new vibration cycle from starting before adequate packing is obtained.

4. Results

Results are obtained for monodispersed systems of spherocylinders to verify the influence of the particle shape on the packing of such particles. The solid fraction of a particle bed is defined as the fraction of its total volume that is occupied by particles. The remaining fraction is called the porosity or void fraction of the bed. Many phenomena that can occur inside a bed depend on these properties, such as the adsorption of molecules in the solid matrix or the flow of a fluid across the interstices. In this section, porosity of monodispersed beds of spherocylinders is studied by means of the Monte Carlo method. For this purpose, aspect ratios ranging from zero to 3.5 are considered. In order to focus on shape effects, all the simulated particles, whose geometric properties are in Table 1, have the same volume ($v = 0{,}5236$ mm^3, equivalent to that of a sphere of 1 mm diameter) and density ($\rho = 10^3$ kg/m^3).

Table 1. Geometric parameters of the simulated particles

Particle Shape	Diameter (mm)	Length (mm)	Aspect Ratio
	1.0000	0.0000	0.000
	0.9443	0.1180	0.125
	0.8993	0.2248	0.250
	0.8298	0.4149	0.500
	0.7778	0.5834	0.750
	0.7368	0.7368	1.000
	0.6751	1.0127	1.500
	0.5949	1.4872	2.500
	0.5429	1.9000	3.500

For each particle type, simulations are performed in cylindrical containers ($D = 12\times10^{-3}$ m and $N_P = 2500$), as well as in boxes with periodic lateral conditions ($L = 10\times10^{-3}$ m and $N_P = 2000$). Initial configurations are generated in *lattice* structures (Abreu, 2002) and then randomized through 10^4 Monte Carlo steps in the absence of gravity. Other simulation conditions are independent on the box type. The granular temperature (T) is set to zero. The fluid density (ρ_f) is 1.0 kg/m^3 and the gravity acceleration (g) is 9.8 m/s^2. Looking at effective packing, 20 shaking steps are simulated using the methodology formerly exposed. Next, the execution of 5×10^4 additional Monte Carlo cycles promotes the final compaction of the bed. For each system, vibrations are performed either with $A_{vib} = 2.0\times10^{-3}$ m or with $A_{vib} = 0.5\times10^{-3}$ m. The other vibration parameters are $N_{min} = 10^3$, $N_{avg} = 10$, and $\delta_E = 10^{-5}$. Three-dimensional visualizations of some obtained configurations are shown in Figure 3.

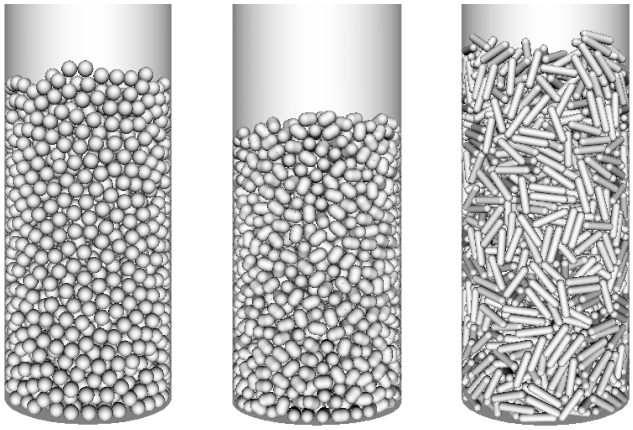

Figure 3. Three-dimensional visualization of simulated beds

For particles with no internal porosity, the solid fraction of a bed could be the ratio between the volume occupied by the particles and the total volume of the bed. However, to avoid the accounting of border (top and bottom) effects, only a central portion of the bed is sampled. This means that only those particles whose centers lie between a height z_{min} and another height z_{max} ($z_{max} > z_{min}$) contribute to the solid fraction. Certainly, there are particles partially inserted in the sampling region, but the method ignores such a possibility. Although it overestimates the contribution of some particles, it does not account the volume of other particles whose centers lie outside the sampling region. This fact maintains the accuracy of the method by error compensation. The adopted criteria for choosing the values of z_{min} and z_{max} are 1) the height of the sampling region is a fixed fraction (ν_b) of that achieved by the packed bed and 2) the height of the discarded regions (both top and bottom) is the same. Additionally, in order to enhance the accuracy, the porosity of a bed is evaluated for several values of ν_b between 0.4 and 0.7 and then a mean-value ($\bar{\varepsilon}$) is computed.

Figure 4 contains the results of porosity for all the simulated beds. The results shown in Figure 4(a) were obtained with $A_{vib} = 2.0\times10^{-3}$ m and those shown in Figure 4(b) were obtained with $A_{vib} = 0.5\times10^{-3}$ m. The circles represent porosities of cylindrical beds, while the squares refer to beds with periodic lateral conditions. Every result is an average took from ten simulations with the same conditions. Their standard deviations are about 0.002. It is clear, from Figures 4(a) and 4(b), that the curves for cylindrical beds are always above those for periodic beds. This shows that the presence of lateral walls hinders the arrangement of the particles and then prevents a system from reaching a high packing density (low void fraction).

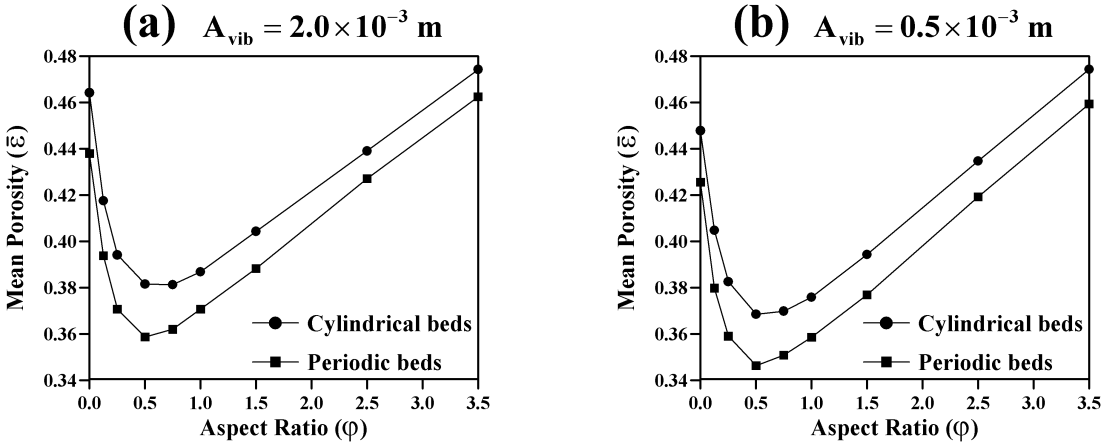

Figure 4. Mean porosity of monodispersed beds of spherocylinders as functions of the particle aspect ratios

Comparing a curve in Figure 4(a) to the corresponding one in Figure 4(b), it is possible to observe that the reduction in the shaking amplitude promotes formation of denser beds, mainly with the less elongated spherocylinders. Although not shown here, an increase in packing densities calculated after consecutive shaking steps (just before the bed lifting) is regularly observed when $A_{vib} = 0.5\times10^{-3}$ m, but it is not observed when $A_{vib} = 2.0\times10^{-3}$ m. Therefore, the smallest amplitude promotes a progressive particle rearrangement, enabling a system to escape from local minima of mechanical energy. On the other hand, with the largest amplitude, the beds practically disassemble and then reassemble in every shaking step.

Another interesting observation in Figure 4 is that all curves present minimum points for particles with aspect ratios of approximately 0.5. This fact can be explained though collective geometric effects. Spherocylinders have additional degrees of freedom, when compared to spheres, due to their axial asymmetry. This enables a more efficient occupation of some irregular gaps that appear inside a bed, reducing its void fraction. However, since the particles are rigid, steric effects become more important as their aspect ratios increase, what enlarges the volume of the interstices and, consequently, increases the void fraction of a bed. In such a manner, the conjunction of these two effects may be responsible for the behavior observed in Figure 4. Zou and Yu (1996) observed similar features in experimental curves of porosity versus sphericity, obtained for monodispersed beds of disks and of cylinders. In the case of spherocylinders, however, experimental data were not found.

It is known that the characteristics of a packed bed depend on the packing conditions. In the case of randomly distributed beds of monosized spheres, measured bulk porosities vary from 0.36 (random-close packing) to around 0.42 (random-loose packing) (Reyes and Iglesia, 1991). This later value was obtained here for laterally periodic beds of spheres after the simulation of vibrations with amplitude equal to 0.5×10^{-3} m, as seen in Figure 4(b) for $\varphi = 0$. This fact suggests that the lowermost curve of Figure 4(b) is the most likely to represent real packed beds of spherocylinders. Anyway, the mean porosity calculated for spherocylinders with $\varphi = 0.5$ ($\bar{\varepsilon} \approx 0.346$) is lower than the typical value achieved by random-close packing of spheres, showing that an actual reduction in void fraction can be obtained by using this kind of spherocylinders in place of spheres. A possible practical application of this result is in the storage of natural gas. As stated by Wegrzyn and Gurevich (1996), one of the problems in using granular solids to store adsorbed natural gas is the lower volumetric efficiency (volume of gas at normal temperature and pressure divided by the volume of the tank) of this process, when compared to the storage by compression. According to the authors, improvement in packing density is a possible way of solving this problem.

5. Conclusions

In this paper, the Monte Carlo method is used for calculating porosities of beds of spherocylinders either confined by cylindrical walls or subject to periodic boundary conditions. These calculations show that the presence of lateral walls can prevent a system from reaching its maximum packing. Another observation is that, for particles with volume equal to 0.5236 mm^3, a reduction in vibration amplitude from 2 mm to 0.5 mm increases the packing density of the beds, mainly for slightly elongated particles. Independently on the box type or shaking amplitude, maximum packing occurs for spherocylinders with aspect ratio approximately equal to 0.5. This result can be useful in the construction of systems for efficient storage of adsorbed natural gas.

6. Acknowledgements

The authors are grateful for the financial support of the Brazilian agencies FAPERJ, CNPq, PRONEX (grant no. 124/96) and PRH-ANP/MCT.

7. References

ABREU, C. R. A., MACIAS-SALINAS, R., TAVARES, F. W., CASTIER, M. Monte Carlo Simulation of the Packing and Segregation of Spheres in Cylinders, *Brazilian Journal of Chemical Engineering*, v. 16, n. 4, p. 395-405, 1999.

ABREU, C. R. A. *Desenvolvimento de Técnicas de Simulação de Sistemas Granulares para Aplicação na Indústria do Petróleo*, Exame de Qualificação ao Doutorado, Escola de Química-UFRJ, 2002.

ALLEN, M. P., TILDESLEY, D. J. *Computer Simulation of Liquids*, Oxford University Press, 1987.

BOLHUIS, P., FRENKEL, D. Tracing the phase boundaries of hard spherocylinders. *Journal of Chemical Physics*, v. 106, n. 2, p. 666-687, 1997.

CASTIER, M., CUÉLLAR, O. D., TAVARES, F. W. Monte Carlo Simulation of Particle Segregation. *Powder Technology*, v. 97, n. 3, p. 200-207, 1998.

MATRANGA, K. R., MYERS, A. L., GLANDT, E. D. Storage of Natural Gas by Adsorption on Activated Carbon. *Chemical Engineering Science*, v. 47, n. 7, p. 1569-1579, 1992.

REYES, S. C., IGLESIA, E. Monte Carlo Simulations of Structural Properties of Packed Beds. *Chemical Engineering Science*, v. 46, n. 4, p. 1089-1099, 1991.

ROSATO, A., PRINZ, F., STANDBURG, K. J., SWENDSEN, R. Monte Carlo Simulation of Particulate Matter Segregation, *Powder Technology*, v. 49, n. 1, p. 59-69, 1986.

VEGA, C., LAGO, S. A Fast Algorithm to Evaluate the Shortest Distance Between Rods. *Comput. & Chem.*, v. 18, n. 1, p. 55-59, 1994.

WEGRZYN, J., GUREVICH, M. Adsorbent Storage of Natural Gas, *Applied Energy*, v. 55, n. 2, p. 71-83, 1996.

ZOU, R. P., YU, A. B. Evaluation of the Packing Characteristics of Mono-Sized Non-Spherical Particles, *Powder Technology*, v. 88, n. 1, p. 71-79, 1996.